Alginate modification scheme

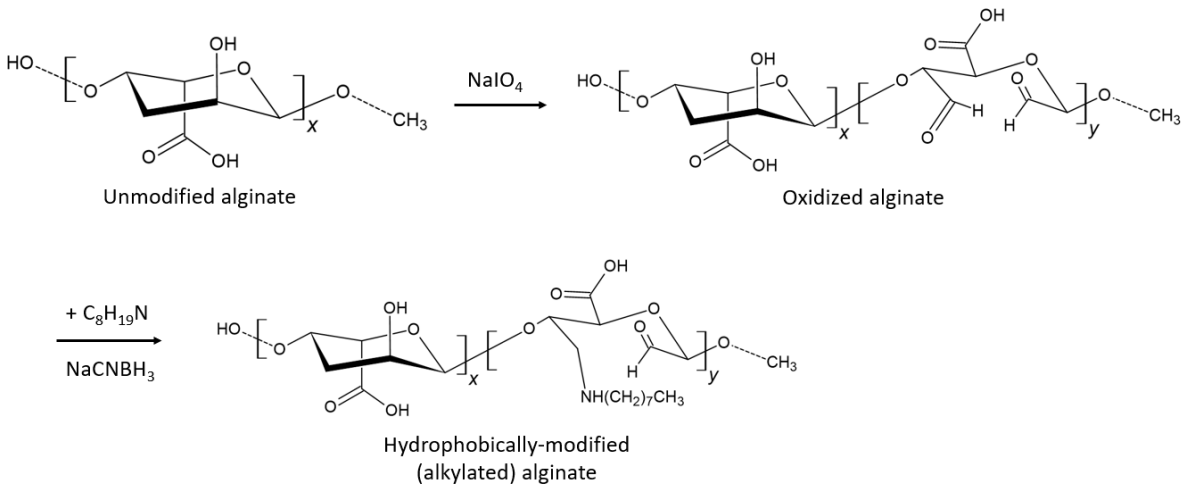

Figure S1: Oxidation-reductive amination reaction scheme for hydrophobic modification of alginate.

Overall composite hydrogel formulation scheme

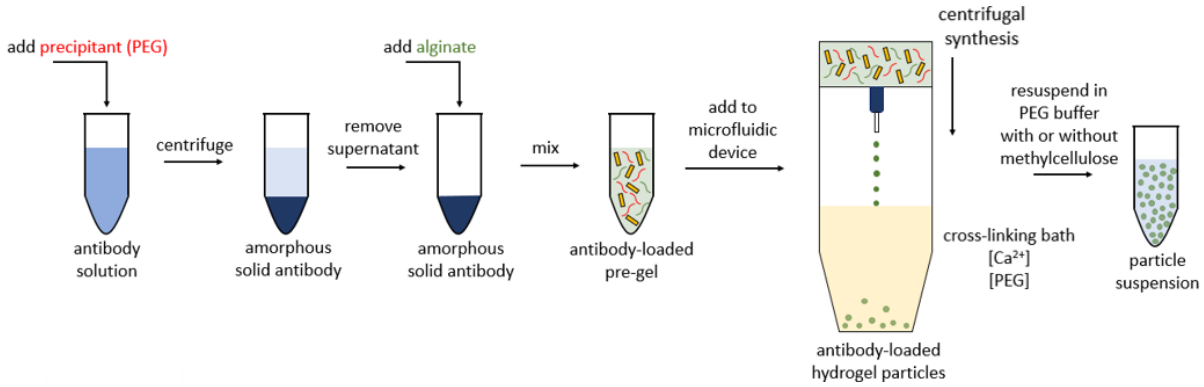

Figure S2: Steps of the formulation process for the alginate-methylcellulose composite hydrogel.

Figure S2 shows the overall formulation process for the composite hydrogel. First, amorphous solid forms of the antibody were prepared via precipitation (recovery = 99.4% ± 0.1). Next, a sodium alginate solution (2% w/v) mixed into the solid antibodies to form the pre-gel, which was then passed through a simple microfluidic device for centrifugal synthesis[1]. In this device, the pre-gel is extruded through a needle by centrifugal force, forming droplets which are collected in a cross-linking bath containing calcium chloride ($CaCl_2$), allowing the alginate to ionically cross-link into hydrogel particles. PEG (10% w/v) is present in both the pre-gel and calcium bath to prevent dissolution of the solid antibodies. Previous works have shown this approach to be a robust and minimal process to prepare antibody-laden alginate

microparticles[2,3]. Finally, to form the composite *in situ* gelling hydrogel, the particles were suspended in a buffer containing 10% w/v PEG and 4% w/v MC. The final dosage form was be prepared using only three gentle steps (precipitation, encapsulation, and suspension), without the use of chemical reactions or an organic phase.

Encapsulation efficiencies for alginate microparticles with different degrees of hydrophobic substitution were measured and are shown below in Table S1.

Table S1. Encapsulation efficiency of IgG ASD-laden alginate microparticles.

Alginate degree of substitution		
0%	3%	6%
99.6% ± 0.1	98.3% ± 0.3	99.9% ± 0.1

Solubility of IgG ASD in methylcellulose

For evaluating the solubility of the amorphous solid antibody in formulations containing methylcellulose to ensure the stability of the solid phase in the composite hydrogels, IgG ASD-laden hydrogel particles were prepared as described earlier. The samples were transferred to a microcentrifuge tube and excess storage buffer was removed to adjust the total IgG content in each tube to 3 mg. 300 μL of storage buffer with different w/v% concentrations of MC were added each tube and the samples were left to equilibrate with the buffer at room temperature (~22^{o}C). After 24 h, the protein concentration in the supernatant was measured using the 280 nm absorbance method.

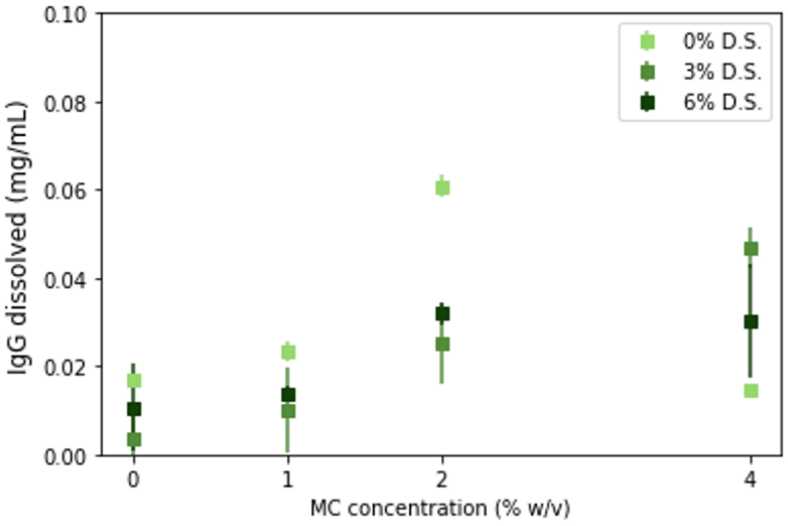

Figure S3: Solubility of IgG (in mg/mL) from alginate (0%, 3%, or 6% degree of substitution) particles suspended in methylcellulose solution.

As in Figure S3, we observe that the solubility of IgG is very low (¡0.1 mg/mL) for all formulations. The solubility of the ASDs are not significantly affected by the presence of methylcellulose in the storage

buffer, which indicates that the majority of IgG (>99%) in the formulations remains in its solid form, and thus encapsulated in the particles. There is no significant 'leakage' of IgG from the particles when stored in 4% w/v methylcellulose solution and the solid form of the antibody is maintained.

Size exclusion chromatography (SEC) of released IgG

Analytical SEC was used to determine the quantity of antibody monomer and aggregates from IgG ASD-laden alginate particles. For this purpose, an AKTA FPLC instrument (GE Healthcare) was used, with a Superdex 200 Increase 10/300 GL analytical SEC column. SEC experiments were carried out at a flow rate of 0.5 mL/min in a phosphate buffered saline (PBS) at pH 7.4. Select conditions were used to characterize the quality of the released IgG antibody in different formulations. For the control experiment, lyophilized IgG powder as received was dissolved into PBS and analyzed. The SEC results are tabulated below in Table S2. Experiments were performed in triplicate (n=3) for each condition, with standard deivations reported.

Table S2. Stability of amorphous IgG evaluated using size exclusion chromatography.

	Monomer %	Aggregates %
Control	81.6 ± 1.0	18.4 ± 1.0
Released from alginate particles, 0% d.s.	84.9 ± 1.5	15.1 ± 1.5
Released from alginate particles, 6% d.s.	82.8 ± 0.9	17.2 ± 0.9
Released from alginate particles in methylcellulose, 0% d.s.	80.2 ± 1.3	19.8 ± 1.3
Released from alginate particles in methylcellulose, 6% d.s.	80.7 ± 0.7	19.3 ± 0.7

As seen in Table S2, the quality of the IgG released from alginate particles is not significantly different from the control (>80% monomer), indicating that IgG remains stable when formulated into the hydrogels, both for alginate alone and in the composite alginate-methylcellulose hydrogel. In addition, the degree of alginate modification does not affect the stability, with 0% d.s. and 6% d.s. alginate hydrogels showing similar monomer compositions across conditions. Characteristic UV traces for each condition are available in Figure S4.

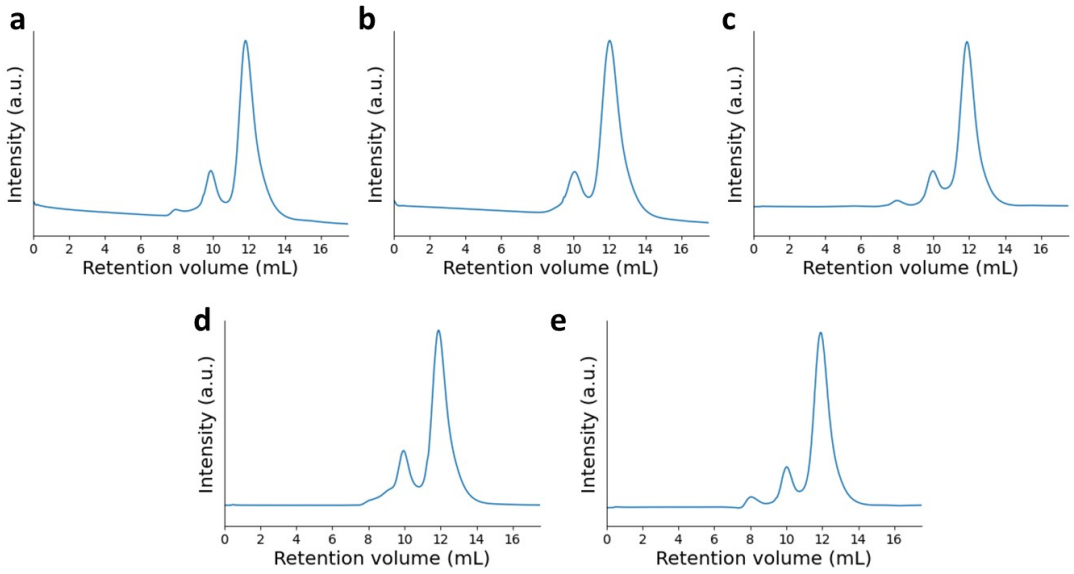

Figure S4: UV traces from size exclusion chromatography of released IgG from (a) control sample, (b) alginate particles, 0% d.s., (c) alginate particles, 6% d.s., (d) alginate particles in methylcellulose, 0% d.s., and (e) alginate particles in methylcellulose, 6% d.s.

Thermoreversibility of MC-alginate mixtures

To demonstrate the thermoreversibility of methylcellulose and alginate composites, the rheological behavior of a MC-alginate solution was characterized using multiple temperature sweep cycles. A temperature ramp was performed on the sample from 20^{o}C to 40^{o}C at a rate of 2^{o}C/min. Between each ramp cycle, the sample was cooled to 20^{o}C and equilibrated for 15 minutes before repeating the same ramp. The results of both cycles are shown below in Figure S5a. The sample has very similar temperature sweep profiles in each run with some small hysteresis. We also performed temperature jump experiments to compliment the temperature ramp data. For thermally gelling soft matter, it is well known in the literature that the evolution of structure (and hence moduli) in a temperature ramp versus temperature jump experiment can differ. Data for temperature jump experiments are show in Figure S5b. The temperature was stepped between 20^{o}C and 40^{o}C for 2 cycles, and each step had a duration τ=30 minutes.

The sol-gel transition of the MC-alginate mixture is reproducible upon cooling, showing the presence of alginate in the solution does not affect methylcellulose's native thermoreversibility. In addition, the sol-gel transition temperatures are not affected by multiple heating/cooling cycles. When gradually heated from 20^{o}C, the MC-alginate solution shows a consistent apparent gelation temperature of ∼37-38^{o}C (Figure S5a). Similarly, as shown in Figure S5b, G'>G" at 40^{o}C while G"<G' at 20^{o}C in both cycles, demonstrating that the sol-gel transition is reversible when alginate is mixed with methylcellulose. The transition from a gel to sol and then sol to gel is quick during temperature jumps. Furthermore, temporal evolution of both the G' and G" curves in the repeated cycles are very similar. The MC-alginate mixture is in solution at room temperature and becomes a semi-solid gel at physiological temperatures across

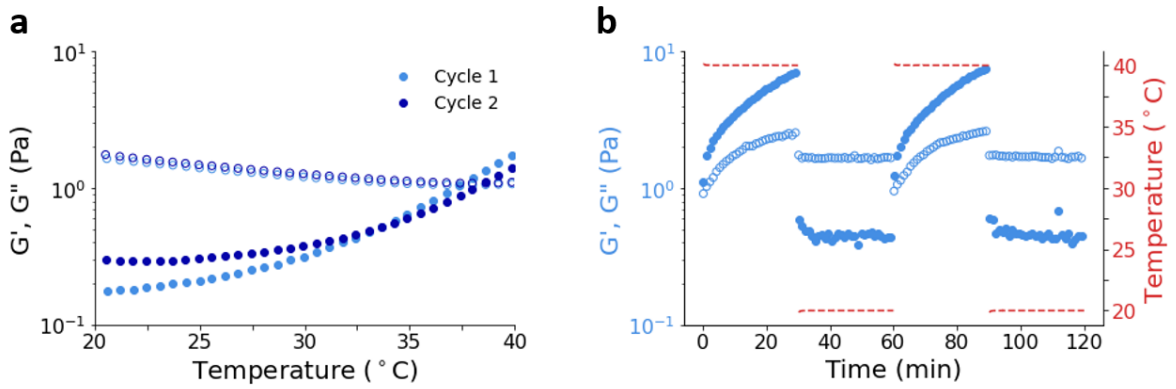

Figure S5: Small amplitude oscillatory shear (a) temperature sweep data for 4% w/v methylcellulose and 1% w/v alginate (0% d.s.) solution with 2 cycles of heating, and (b) time sweep data for 4% w/v methylcellulose and 1% w/v alginate (0% d.s.) solution with 2 cycles of heating and cooling. (•) denotes storage modulus (G'), (○) denotes loss modulus (G"), and - - - denotes temperature. The temperature and time sweeps were performed at a strain amplitude of 1% and frequency of 1.6 Hz

multiple cycles, indicating its reversibility and suitability for pharmaceutical applications. We also see that the storage modulus increases over time when the sample is held at 40^oC, indicating the formation of a stronger gel over time which may lend to the release behavior of the *in situ* gel as discussed.

Drug release model fitting

To fit the release profiles presented in this work, the Weibull model was used. Though the Peppas (power-law) model (Equation S1) is more frequently applied for drug release from hydrogel-based delivery systems, it is a short-time approximation (valid for $M_t/M_\infty \leq 0.60$). Thus, the Peppas model does not provide a good fit across the entire release profile.

$$\frac{M_t}{M_\infty} = kt^n \tag{S1}$$

However, the value of the model exponent (n) in the Peppas model can provide a better physical and kinetic basis than the Weibull model[4]. The interpretation of n is similar to that of b in the Weibull model, such that n≤0.43 indicates a diffusion-controlled, first-order release mechanism, n>0.85 indicates a polymer erosion-controlled, zero-order release profile, and values of n between 0.43 and 0.85 indicate anomalous transport in between the two limits[5]. For the purposes of comparison, the exponent values for both the Weibull and Peppas model and their fit (R^2) across the entire range of release data are shown in Table S3. As we see in Table S3, the value of b generally corresponds with the value of n, suggesting good agreement of the release mechanism regimes and a valid basis for the Weibull model used in the main work.

Table S3. Drug release model parameters and fits for the Weibull and Peppas models.

	Formulations without methylcellulose				Formulations with methylcellulose			
	Weibull model		Peppas model		Weibull model		Peppas model	
	b	R^2	n	R^2	b	R^2	n	R^2
ASD only	5.02	0.999	n/a*		0.54	0.981	0.30	0.737
Pre-gel, 0% d.s.	6.56	0.999	n/a*		1.93	0.988	0.56	0.844
Pre-gel, 3% d.s.	0.51	0.988	0.29	0.946	0.722	0.991	0.52	0.878
Pre-gel, 6% d.s	2.59	0.999	1.70	0.758	0.779	0.979	0.47	0.969
Particles, 0% d.s.	0.727	0.990	0.40	0.978	1.13	0.978	0.79	0.861
Particles, 3% d.s.	0.838	0.990	0.56	0.986	0.962	0.992	0.66	0.850
Particles, 6% d.s.	1.16	0.991	0.76	0.938	1.07	0.995	0.76	0.866

*Peppas model was not valid here as all data points in this profile were $M_t/M_\infty > 0.60$

Multiple sample replicates of *in vitro* release tests

Select alginate particle formulations, with and without methylcellulose, were chosen to demonstrate consistent control in *in vitro* release kinetics across multiple samples of the same formulation conditions, whereas the data in the main text (Figure 3) is taken as technical replicates. *In vitro* release tests were performed for multiple samples (n=3) of select formulation conditions. The results are shown below in Figure S6.

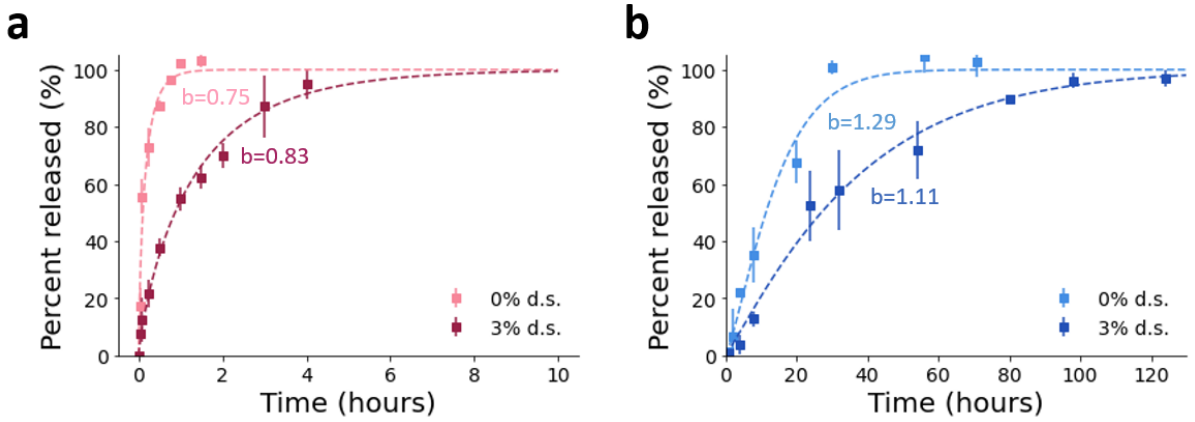

Figure S6: Profiles of *in vitro* release tests performed in simulated bodily fluid, with dashed lines fitted to the Weibull model for the averaged data, for ASD-laden alginate (2% w/v) microparticles (a) suspended in buffer with 0% (R^2=0.965) and 3% (R^2=0.991) degree of alginate substitution, and (b) suspended in buffer with 4% w/v methylcellulose with 0% (R^2=0.986) and 3% (R^2=0.991) degree of alginate substitution. Data are shown for multiple sample replicates, n=3, and error bars show standard deviation.

In general, we find consistent release kinetics across different samples in each of the formulation conditions and show that trends in release behavior remain the same, as according to the value of b in the

Weibull model fits. As discussed in the main text, the b values for formulations without methylcellulose can be controlled by the degree of alginate substitution, going from the diffusion-controlled release regime ($b \leq 0.75$) in the case of the unmodified alginate particles to approaching the erosion-controlled regime as the value of b increases with degree of alginate substitution. For the formulations with methylcellulose, all profiles again show release behavior within the erosion-controlled release regime ($b > 1$) regardless of the degree of alginate substitution. The individual Weibull and Peppas fits for each of the replicated samples are reported below in Table S4.

Table S4. Drug release model parameters and fits for the Weibull and Peppas models.

	Formulations without methylcellulose				Formulations with methylcellulose			
	Weibull model		Peppas model		Weibull model		Peppas model	
	b	R^2	n	R^2	b	R^2	n	R^2
Particles, 0% d.s.	0.727	0.990	0.40	0.978	1.13	0.978	0.79	0.861
	0.782	0.936	0.53	0.795	1.34	0.967	0.80	0.886
	0.795	0.950	0.55	0.771	1.45	0.996	0.90	0.720
Particles, 3% d.s.	0.838	0.990	0.56	0.986	0.962	0.992	0.66	0.850
	1.01	0.982	0.49	0.913	1.07	0.949	0.72	0.877
	0.875	0.931	0.49	0.961	1.15	0.988	0.79	0.940

Injectability test set-up

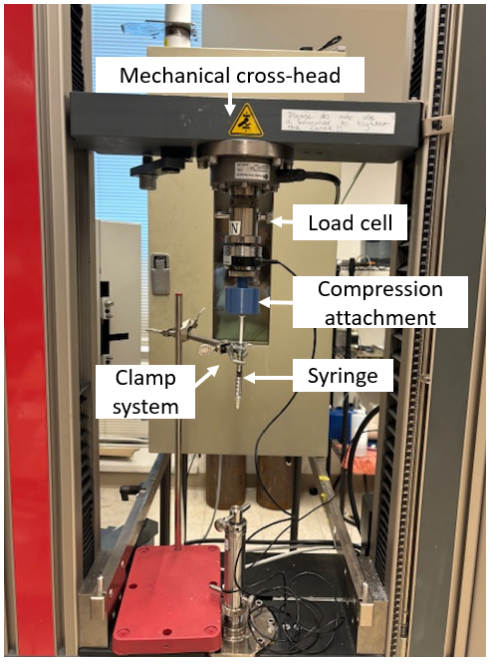

Figure S7: Image of the set-up for the injectability tests, displayed at the beginning of a test.

References

[1] H. B. Eral, E. R. Safai, B. Keshavarz, J. J. Kim, J. Lee and P. S. Doyle, *Langmuir*, 2016, **32**, 7198–7209.

[2] A. Erfani, J. M. Schieferstein, P. Reichert, C. N. Narasimhan, C. Pastuskovas, V. Parab, D. Simmons, X. Yang, A. Shanker, P. Hammond and P. S. Doyle, *Advanced Healthcare Materials*, 2022, **n/a**, 2202370.

[3] A. Erfani, P. Reichert, C. N. Narasimhan and P. S. Doyle, *iScience*, 2023, **26**, 107452.

[4] V. Papadopoulou, K. Kosmidis, M. Vlachou and P. Macheras, *International Journal of Pharmaceutics*, 2006, **309**, 44–50.

[5] P. L. Ritger and N. A. Peppas, *Journal of Controlled Release*, 1987, **5**, 37–42.